Chapter 7.2

PHENOLOGY OF VEGETATION PHOTOSYNTHESIS

Lianhong Gu[1], Wilfred M. Post[1], Dennis Baldocchi[2], T. Andy Black[3], Shashi B. Verma[4], Timo Vesala[5], and Steve C. Wofsy[6]

[1]Environmental Sciences Division, Oak Ridge National Laboratory, Oak Ridge, TN, USA; [2]Department of Environmental Science, Policy & Management, University of California, Berkeley, CA, USA; [3]Faculty of Agricultural Sciences, University of British Columbia, Vancouver, Canada; [4]School of Natural Resource Sciences, University of Nebraska, Lincoln NE, USA; [5]Department of Physical Sciences, University of Helsinki, Helsinki, Finland; [6]Department of Earth and Planetary Sciences, Harvard University, Cambridge, MA, USA

Key words: Photosynthesis, Phenological indices, Vegetation, Eddy covariance, Ecosystems

1. INTRODUCTION

Traditionally, the study of plant phenology focuses on monitoring and analyses of the timing of life-cycle events. In phenological observations, one of the most important tools has been our eye. Consequently, the life-cycle events that are subject to most phenological investigations have been those that are easily visible, e.g. leaf bud break, first flowering, leaf coloring, leaf fall, etc. Although plant scientists have been always interested in the physiological bases that control the phenological stages of plants (e.g., Mott and Mccomb 1975; Suárez-López et al. 2002; Yanovsky and Kay 2002), analyses and prediction of the timing of these visible events have dominated phenological studies in the past (e.g., Lieth 1974; Podolsky 1984; Peñuelas and Filella 2001). In conjunction with this feature of "visibility", traditional phenological studies are also characterized by "individuality" in the sense that individual species instead of plant communities are subject to

Schwartz (ed.), PHENOLOGY: AN INTEGRATIVE ENVIRONMENTAL SCIENCE, 467-485

observations, and "discontinuity" in the sense that the observational time domain is discontinuous (often once a year).

These legacies in past phenological studies need a careful look. Our ability to predict a phenological event will eventually depend on how well the biological mechanism is understood. Visible life-cycle events are results and external exhibitions of internal plant physiological processes that operate under changing environmental conditions. They represent the structural aspects of plant activities. Equally revealing about the underlying processes are changes in the functional aspects of plant activities, in particular, the exchanges of mass and energy between plants and their environment (e.g., Fitzjarrald et al. 2001; Freedman et al. 2001; Schwartz and Crawford 2001). These functional aspects of plant activities, although not visible, provide quantitative measures of plant responses to changes in environmental conditions and thus are important for the study of phenology.

Shifts in the timing of phenological events serve as powerful biological indicators of global climate change. While targeting individual species makes visual observation easier, phenological responses to environmental changes are species-specific (e.g., Bradley et al. 1999; Spano et al. 1999; Peñuelas and Filella 2001). This makes the comparison of changes in the ontogenetic development of different plants in response to climate changes difficult. Efforts have been made to use cloned plants to obtain comparable phenological data across different regions (Schwartz 1994; Chmielewski 1996; Menzel and Fabian 1999). Although cloned plants help eliminate uncertainty due to genetic variability, species adaptation to local climates may bring additional uncertainty to phenological comparisons in different climatic regions. Eventually the use of cloned plants will be limited by their biogeographical distributions. These potential difficulties with individual plant species point to the need for also using responses of a collection of plant species or plant communities as indicators of climate change.

How plants reach from one life-cycle event to another is a topic hard to deal with within the traditional framework of plant phenology because of its focus on discontinuous life-cycle events. However, plant lives are not just composed of individual events but also continuous responses and feedbacks to the ever-changing environmental conditions. To understand precisely how environmental variables affect plant life-cycle events, plant-environment interactions over the whole time domain must be considered. In this regard, continuous measurements of exchanges of mass and energy between plants and their environment provide valuable information about plant activities between life-cycle events.

Today's expanded interest in phenology stems from the realization of the potential roles that phenology can play in monitoring and understanding biospheric responses to global climate change. This new application of

phenology calls for new dimensions and new tools in phenological studies. To this end, establishing a linkage between traditional phenology and terrestrial biophysics is of critical importance. Such a linkage is needed because the interactions between vegetation and atmosphere are realized through various biophysical fluxes (carbon dioxide, water vapor, sensible heat, etc) that transfer between them, and these biophysical fluxes are affected by phenological events (Baldocchi et al. 2001; Fitzjarrald et al. 2001; Freedman et al. 2001; Schwartz and Crawford 2001).

In this chapter, we take an ecosystem-level functional approach to phenological studies. Instead of focusing on life-cycle events of individual plants, we explore seasonal demarcations in canopy photosynthesis, which contain rich information about plant phenology. Instead of basing our analysis on individual species, we use plant communities (vegetation canopies) as our observational subjects. Such a community-based approach complements the traditional species-based approach in the sense that the former captures the broad vegetational responses while the latter reveals the sensitive changes of individual species. We are interested in not only the timing of individual phenological events but also how communities change from one event to another. Our objective is to develop a systematic methodology that can be used to extract phenological information on photosynthesis from continuous measurements of net ecosystem exchanges (NEE) of carbon dioxide (CO_2). We derive a series of phenological indices that can be used to characterize seasonal patterns of vegetation photosynthesis. Our observational tool is the eddy covariance method, a micrometeorological technique that measures trace gas fluxes between the biosphere and atmosphere. Although transitions in surface energy balance are closely related to leaf phenology, and it is possible to extract phenological information from energy flux measurements also (Baldocchi et al. 2001; Fitzjarrald et al. 2001; Schwartz and Crawford 2001), this chapter focuses on the CO_2 flux only because of the current emphasis on the global carbon cycle by the global change community.

In the following sections, we first introduce the eddy covariance technique and the available flux dataset. Then we outline the model that is used to infer canopy photosynthetic rates from NEE measurements. From there we describe how canopy photosynthetic rates can be used to characterize phenology on a plant community level.

2. EDDY COVARIANCE FLUX MEASUREMENTS

The eddy covariance technique measures vertical flux densities of scalars (e.g., CO_2, water vapor, temperature) between ecosystems and the

atmosphere by determining the mean covariance between the vertical wind velocity and the respective scalar fluctuations. Typical instrumentation at an eddy covariance site includes a three-dimensional sonic anemometer, to measure wind velocities and virtual temperature, and a fast responding sensor to measure CO_2 and water vapor. Scalar concentration fluctuations are measured with open and closed path infrared gas analyzers. Over short canopies, these sensors can be mounted on small poles, while walk-up scaffolding or low-profile radio towers are used over forest canopies. Sampling rates between 10 and 20 Hz ensure complete sampling of the high frequency portion of the flux co-spectrum. The sampling duration must be long enough to capture low frequency contributions to flux covariance, but not too long to be affected by diurnal changes in temperature, humidity and CO_2. Adequate sampling duration and averaging period vary between 30 and 60 minutes for most teams. Regular calibrations of gas analyzers are needed to correct potential instrument zero and span drifts. For further information on the eddy covariance method, readers are referred to Baldocchi et al. (1988) and Aubinet et al. (2000).

There are now over 200 eddy covariance flux tower sites operating on a long-term and continuous basis globally. At most sites, researchers also collect data on site vegetation, soil, hydrologic, and meteorological characteristics. Regional and global networks have been formed with the aim to understand the mechanisms controlling the flows of CO_2, water, and energy to and from the terrestrial biosphere across the spectrum of time and space scales. Data compiled by these flux networks are freely available to the science community through the internet and provide unique opportunities to study biophysical aspects of plant community phenology. Further information on these flux networks and available datasets can be found at http://public.ornl.gov/ameriflux, or http://www-eosdis.ornl.gov/FLUXNET.

3. INFERRING VEGETATION PHOTOSYNTHESIS

The eddy covariance method measures NEE, which is composed of two components: canopy photosynthetic flux density (gross photosynthesis, P_g) and ecosystem respiration rate (R_e):

$$N_e = R_e - P_g \tag{1}$$

where N_e denotes NEE of CO_2. R_e consists of carbon flux from autotrophs (leaves, roots, and shoots of plants) and heterotrophs (microbes, fungi, bacteria, etc.) to the atmosphere. For phenological studies, it is desirable to

analyze P_g instead of N_e or R_e since P_g is more directly related to plant community activities. We apply the model of Gu et al. (2002) to infer P_g from measured N_e. In Gu et al. (2002), the following function is used to express the dependence of P_g on diffuse photosynthetically active radiation (diffuse PAR, I_f) and direct photosynthetically active radiation (direct PAR, I_r):

$$P_{\mathrm{g}} = \frac{(\alpha_{\mathrm{f}} I_{\mathrm{f}} + \alpha_{\mathrm{r}} I_{\mathrm{r}})(\beta_{\mathrm{f}} I_{\mathrm{f}} + \beta_{\mathrm{r}} I_{\mathrm{r}})}{(\beta_{\mathrm{f}} I_{\mathrm{f}} + \beta_{\mathrm{r}} I_{\mathrm{r}}) + (\alpha_{\mathrm{f}} I_{\mathrm{f}} + \alpha_{\mathrm{r}} I_{\mathrm{r}}) I_{\mathrm{t}}} \tag{2}$$

where α_f and α_r are the initial canopy quantum yield for diffuse and direct PAR, respectively; β_f and β_r are the closeness to linear response (CLR) coefficient for diffuse and direct PAR, respectively; I_t is global PAR (= I_f + I_r). Equation (2) is a generalization to the rectangular hyperbola model commonly used in flux analyses (see references in Gu et al. 2002). The advantage of Equation (2) over the traditional rectangular hyperbola model is that it can describe the differential canopy photosynthetic responses to diffuse and direct PAR. Gu et al. (2002) compared the new model with the traditional rectangular hyperbola for a variety of vegetation sites and found that the new model provides a better fit to observations. The dependence of R_e on temperature is described by the following function:

$$R_e = c_1 e^{c_2[c_3 T_a + (1-c_3)T_s]} + d_1 e^{d_2 T_s} \tag{3}$$

where c_1, c_2, c_3, d_1 and d_2 are regression coefficients; T_s is soil temperature; T_a is air temperature.

With measured N_e and Equations (1)-(3), parameters in (2) and (3) can be estimated through nonlinear regression. To obtain P_g, estimated α_f, α_r, β_f and β_r are used in (2). Equation (3) can be used to estimate R_e from fitted values of c_1, c_2, c_3, d_1 and d_2 (R_e is not used in this study).

4. SEASONAL PHOTOSYNTHETIC PATTERNS OF CONTRASTING TERRESTRIAL ECOSYSTEMS

We have used the method described in the previous section to infer canopy photosynthetic rates for five sites with contrasting vegetation structures and climatic conditions. These sites are a Scots pine forest in Hyytiälä, Finland (61°51'N, 24°17′E, data from 1997), an aspen forest in

Prince Albert National Park, Saskatchewan, Canada (53°63′N, 106°20′W, 1996), a mixed deciduous forest in Walker Branch Watershed, Tennessee, USA (35°58′N, 84°17′W, 1996), a mixed hardwood forest in Massachusetts, USA (Harvard Forest, 42°32' N, 72°10'W, 1992), and a native tallgrass prairie in Oklahoma, USA (36°56′N, 96°41′W, 1997). Detailed site information can be found elsewhere (Goulden et al. 1996; Gu et al. 2002, and references therein).

Since diurnal variations in canopy photosynthetic rates do not provide phenological information, we focus on seasonal patterns. Seasonal patterns are characterized by daily maximum canopy photosynthetic rates (P_m). To determine P_m, canopy photosynthetic rates P_g (time step is hourly at the Harvard Forest site, and half-hourly at other sites) in each day are ranked, and the largest value is taken as P_m. For a given site, daily maximum canopy photosynthetic rates form the upper boundary in the scatter plot of canopy photosynthetic rates against time. A few daily maximum values clearly fall out of seasonal patterns due to excessive cloudiness. They can be easily picked up visually. The total number of these points is very small, and they are excluded from the analysis. Figure 1 depicts the seasonal changes of P_{m} at these five sites (unusually small P_m points have been already removed).

Also shown in Figure 1 are values calculated from the Weibull function fitted to these data. This curve fitting is necessary for the determination of phenological indices in the next section. The Weibull function is given as:

$$\begin{cases} P_m(t) = y_0 + a\left(1 - e^{-\left[\frac{\left|t - t_0 + b(\ln 2)^{1/c}\right|}{b}\right]^c}\right), & t \geq t_0 - b(\ln 2)^{1/c} \\ P_m(t) = 0, & t < t_0 - b(\ln 2)^{1/c} \end{cases} \tag{4}$$

where $P_m(t)$ is the daily maximum canopy photosynthetic rate for day t; y_0, t_0, a, b and c are regressional coefficients. Because the Weibull function is monotonic (that is, P_m keeps increasing with t), the fitting has to be done separately for spring and fall. The choice for the end day of the spring portion or the start day for the fall portion does not critically affect the fitting parameters as long as they are within the period in which P_m is relatively constant in the middle growing season. In the fall fitting, the number of days from the end of the calendar year is used as the independent variable. SigmaPlot has a built-in nonlinear regression for the Weibull function and is used in this study.

Our choice of the Weibull function results from many trials and failures. This function fits to observations better than other ones we have tried (e.g., sigmoid). It provides a very good fit at all five sites even through the sites

are quite different in vegetation types. The R^2 of the spring fitting and fall fitting are 0.96 and 0.94 for Harvard Forest, 0.99 and 0.99 for the tallgrass prairie, 0.98 and 0.97 for the Scots pine forest, 0.98 and 0.97 for the mixed forest in Tennessee, and 0.98 and 0.98 for the aspen forest, respectively.

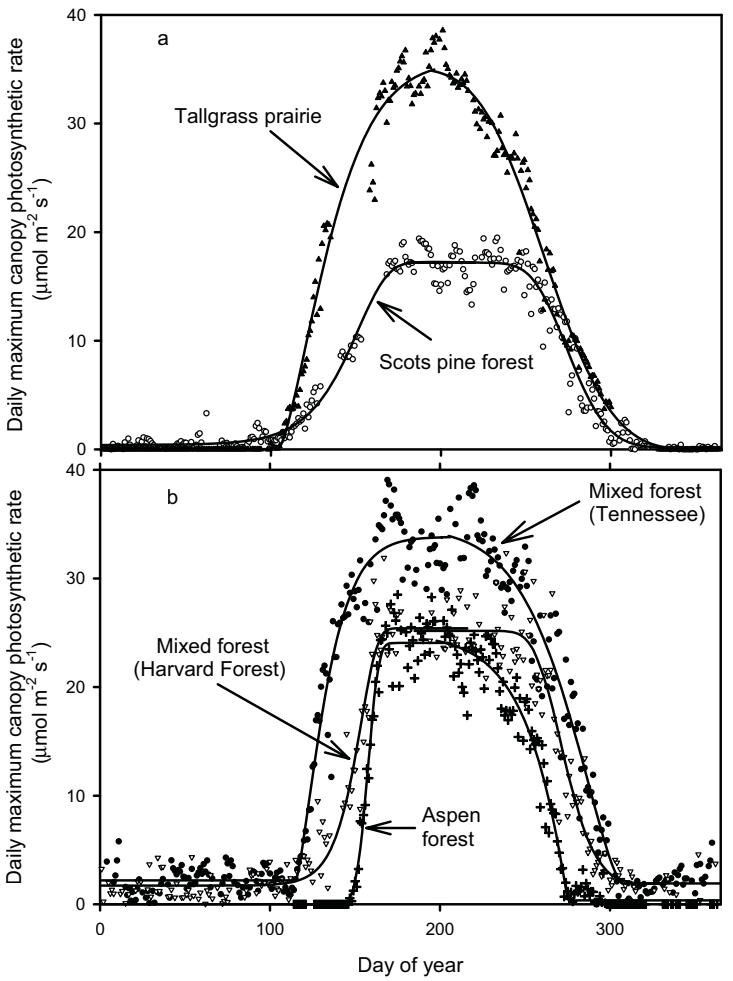

Figure 7.2-1. Seasonal patterns of daily maximum canopy gross photosynthetic rates at five eddy covariance flux sites.

The seasonal patterns in P_m show both differences and similarities among the sites. For example, the growing season of the Scots pine forest almost coincides with that of the tallgrass prairie even through the two sites are nearly 25 degrees (in latitude) apart from each other. However, photosynthesis in the tallgrass prairie increases faster in the spring and reaches a higher maximum rate than does the Scots pine forest. The former starts to decline earlier, leading to a shorter middle growing season when P_m is relatively stable. The three deciduous forests have different growing season lengths, with the aspen forest being the shortest. This is not surprising since the aspen forest site is the most northern of the three sites. However, photosynthesis in the aspen forest increases rapidly in the spring, leading to a middle-growing season photosynthetic peak similar to Harvard Forest's.

These seasonal photosynthetic patterns reflect the responses of plant communities to seasonal cycles in climate conditions. Studying the relationships between the seasonal photosynthetic patterns and climate conditions can yield important insights into how terrestrial ecosystems will respond to global climate changes. However, currently we lack systematic approaches to objectively quantify these seasonal patterns. For example, growing season length has been found to be an important indicator of annual carbon sequestrations (Baldocchi et al. 2001). But how is the growing season defined? As shown in Figure 1, entering into the growing season is a gradual process. Determining the initiation or end day of the growing season can be subjective. Also, two plant communities may have the same growing season length, but differ dramatically in their canopy photosynthetic rates within the growing season (Figure 1a). Therefore, it is desirable to develop a methodology and a set of phenological indices that can be used to objectively and quantitatively characterize the overall patterns of seasonal photosynthetic dynamics of plant communities.

5. PHENOLOGICAL INDICES OF VEGETATION PHOTOSYNTHESIS

Here we introduce a number of indices to quantify seasonal photosynthetic patterns. These indices include: spring photosynthesis development velocity, fall photosynthesis recession velocity, growing season initiation day, growing season termination day, center day of the growing season, length of the growing season, effective length of the growing season, effective daily maximum canopy photosynthetic rate, and seasonal carbon dioxide assimilation potential index. Figure 2 uses Harvard Forest (Figure 2a) and Scots pine forest (Figure 2b) as examples to illustrate these indices.

5.1 Spring Photosynthesis Development and Fall Photosynthesis Recession Velocities

Daily maximum canopy photosynthetic rates, P_m, tend to change linearly with time in spring and fall at all five sites (Figures 1, 2). These linear trends make it possible to define a spring photosynthesis development velocity (V_s, μmol/m^2 s day) and a fall photosynthesis recession velocity (V_f, μmol/m^2 s day), which represent the slopes of the two time periods, respectively. These two pace parameters should contain important information about the response of vegetation to changes in climate conditions. The key is to determine when the linear segments start and when they end.

To do so, we note that the seasonal pattern of P_m shows four sharp turning points with two points in the spring and the other two in the fall. The first sharp turning point in the spring represents the day when canopy photosynthesis development starts to accelerate in response to the rapid improvement in meteorological conditions for plant growth. This day is termed photosynthesis upturn day (PUD, denoted by D_u). The second sharp turning point in the spring corresponds to the day when the development process of canopy photosynthesis starts to slow down and gradually move towards stabilization in which P_m reaches its peak. This day is termed photosynthesis stabilization day (PSD, denoted by D_s). The spring linear segment lies between PUD and PSD.

The first sharp turning point in the fall corresponds to the day when canopy photosynthesis enters into a period of quick decline in response to the deterioration in meteorological conditions for plant growth. This day is termed photosynthesis downturn day (PDD, denoted by D_d). As the recession approaches the end of the growing season, the speed of recession tends to decrease, possibly due to residual photosynthesis by some leaves or conifer species in the plant community, leading to a second sharp turning point in the fall. After the second sharp turning point in the fall, photosynthesis of deciduous trees proceeds to stop while evergreen species may still maintain a low level, limited photosynthetic rate. This second turning point is termed photosynthesis recession day (PRD, denoted by D_r).

These sharp turning points can be located by calculating the radius of curvature of $P_m(t)$. The radius of curvature measures the sharpness that a curve turns. For a given point on a curve, the radius of curvature is the radius of the circle that fits or "kisses" the curve at that point. The more sharply the curve turns, the smaller the radius of curvature is, and vice versa. Mathematically, for curve $f = P_m(t)$, its radius of curvature is $\rho(t)$. The

$$\rho = \frac{\left[1+\left(\frac{dP_m}{dt}\right)^2\right]^{1.5}}{\frac{d^2P_m}{dt^2}} \tag{5}$$

sharpest turning points of curve $P_m(t)$ correspond to the local minima of $\rho\,(t)$ (for details on radius of curvature, consult a calculus textbook such as Thomas and Finney 1998, p. 881-893).

It is possible to determine the radius of curvature from the calculated P_m directly. However this would require a rigorous smoothing procedure to remove the noises in the numerical first and second order derivatives of the calculated P_m. Here we use the fitted Weibull function (4) as shown in Figures 1 and 2. The first and second derivatives of P_m(t) are given by:

$$\frac{dP_m}{dt} = \frac{ac}{b}e^{-k^c}k^{c-1} \tag{6a}$$

$$\frac{d^2P_m}{dt^2} = \frac{dP}{dt}\left(c-1-ck^c\right)\frac{1}{bk} \tag{6b}$$

$$\text{if } k = \frac{t-t_0+b(\ln 2)^{1/c}}{b} \geq 0\text{; and}$$

$$\frac{dP_m}{dt} = 0 \tag{6c}$$

$$\frac{d^2P_m}{dt^2} = 0 \tag{6d}$$

if $k < 0$.

Substituting Expressions (6) into (5) leads to ρ as a function of day of year. Although we could determine the minima of ρ by letting $d\rho/dt = 0$ and solving the resulted complicated third order differential equation, it does not have to be done in this way. We can determine the days when the minimum

ρ occurs by simply ranking the ρs calculated for all days in the year and selecting those days when ρ reaches a minimum.

The two points ($P_m(D_u)$, D_u) and ($P_m(D_s)$, D_s) form a line, which we call "Spring Development Line." The slope of the spring development line, that is, the spring photosynthesis development velocity is given by:

$$V_s = \frac{P_m(D_s) - P_m(D_u)}{D_s - D_u} \tag{7}$$

Similarly, the "Fall Recession Line" is formed by the two points ($P_m(D_d)$, D_d) and ($P_m(D_r)$, D_r). The fall photosynthesis recession velocity is determined by:

$$V_f = \frac{P_m(D_d) - P_m(D_r)}{D_r - D_d} \tag{8}$$

5.2 Growing Season Initiation and Termination Days

We define the intersection between the spring development line and the time (day of year) axis as the initiation of the growing season (see Figure 2). It is easy to show that the growing season initiation day (D_i) is:

$$D_i = \frac{D_u * P(D_s) - D_s * P(D_u)}{P(D_s) - P(D_u)} \tag{9}$$

In a similar fashion, we define the growing season termination day (D_t) as the intersection between the fall recession line and the time axis:

$$D_t = \frac{D_r * P(D_d) - D_d * P(D_r)}{P(D_d) - P(D_r)} \tag{10}$$

The length of the growing season (L) is simply:

$$L = D_t - D_i \tag{11}$$

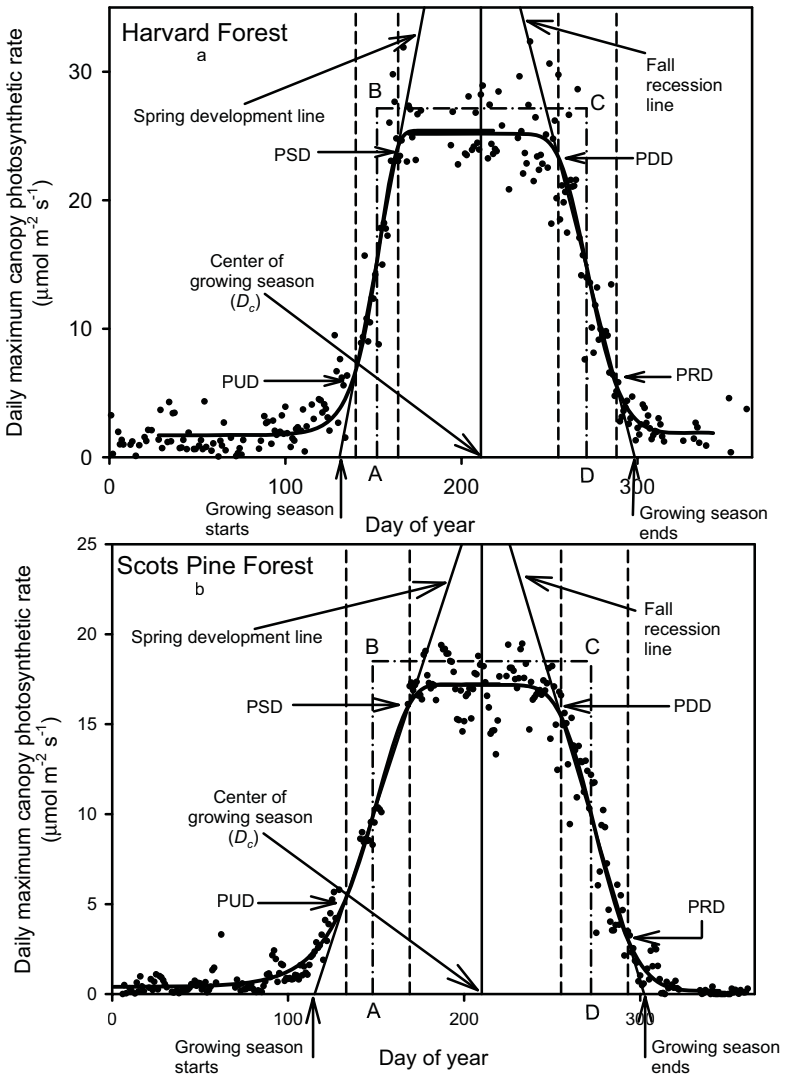

Figure 7.2-2. Determination of phenological indices of vegetation photosynthesis. See text for explanation.

5.3 Center Day and Effective Length of the Growing Season

We define the center day of the growing season (D_c) as the "center of gravity" of the seasonal photosynthesis curve $P_m(t)$:

$$D_c = \frac{1}{w^2}\int_{D_i}^{D_t} tP_m^2 dt \tag{12}$$

where:

$$w^2 = \int_{D_i}^{D_t} P_m^2 dt \tag{13}$$

Center day of the growing season is marked in Figure 2.

The effective length of the growing season (L_e) is defined as the standard deviations from the center day of the growing season D_c:

$$L_e = \frac{2\sqrt{3}}{w}\left[\int_{D_i}^{D_t}(t-D_c)^2 P_m^2 dt\right]^{1/2} \tag{14}$$

where the factor $2\sqrt{3}$ is introduced so that the effective length of the growing season would equal exactly the width of the rectangle if the seasonal pattern of vegetation photosynthesis is perfectly rectangular. In Figure 2(a and b), the number of days between the two points A and D is the effective length of the growing season.

5.4 Seasonal Carbon Assimilation Potential Index and Effective Maximum Canopy Photosynthetic Rate

Let

$$u = \int_{D_i}^{D_t} P_m(t)dt \tag{15}$$

where u is simply the area under the curve $P_m(t)$ within the growing season (see Figure 2). It is an indicator of seasonal carbon dioxide assimilation potential by a canopy under a give climate condition. We call it the seasonal carbon assimilation potential index.

The effective daily maximum canopy photosynthetic rate (P_e) is calculated from the effective length of the growing season L_e and the seasonal carbon assimilation potential index u:

$$P_e = \frac{u}{L_e} \tag{16}$$

In Figure 2(a and b), the height of the rectangular ABCD is P_e.

In this section, we have introduced a series of indices and the methods to determine their values without much elaborating their usefulness. This is the task of the next section.

6. EVALUATION OF PHENOLOGICAL INDICES OF VEGETATION PHOTOSYNTHESIS

With the phenological indices introduced above, seasonal photosynthetic patterns can be quantified and compared among different vegetation types (Table 1). Of course, these indices can change from year to year, in response to interannual climatic variability. Here we do not intend to study such variability, but rather we compare the values of these indices for different sites to illustrate their usefulness.

For the three deciduous forests, the time when the growing season starts and terminates follows the order of their latitudes. However, this pattern does not hold when different functional types are considered. The Scots pine forest in Finland starts to grow almost as early as does the mixed deciduous forest in Tennessee, USA, although the former is a more northern site. The tallgrass prairie site in Oklahoma, USA and the mixed deciduous forest in Tennessee have similar latitudes. However, the growth of the tallgrass prairie is initiated eight days earlier and ends only three days earlier than the mixed deciduous forest in Tennessee.

Clearly for different vegetation functional types, the growing season length is not an indicator of carbon assimilation capacity. The tallgrass prairie in Okalahoma has a longer growing season than the mixed deciduous forest in Tennessee. However, the latter has a higher growing season assimilation potential index than the former even through their effective daily maximum canopy photosynthetic rates are similar. In this regard, the effective length of the growing season depicts the difference between the two sites better. Although the prairie site has a longer growing season, its effective length of growing season is shorter than is the mixed deciduous

forest in Tennessee. Nevertheless for the three deciduous forests, both the length of the growing season and the effective length of the growing season follow the same rank order.

Table 7.2-1. Phenological indices of vegetation photosynthesis determined for the five sites under investigation

Vegetation	Scots Pine Forest	Aspen Forest	Tall grass Prairie	Mixed forest (TN)	Mixed forest (Harvard)
Growing season initiation day (D_i)	116	148	105	113	131
Growing season termination day (D_t)	303	276	308	311	299
Growing season length (L, days)	187	128	203	198	168
Growing season center (D_c)	210	205	197	202	211
Growing season assimilation potential index (u, μmol m^{-2} s^{-1} day)	2290.5	2367.7	4397.6	4760.3	3226.2
Effective growing season length (L_e, days)	124	96	123	136	119
Effective daily maximum canopy photosynthetic rate (P_e, μmol m^{-2} s^{-1})	18.5	24.7	35.8	35.2	27.1
Photosynthesis development velocity (V_s, μmol m^{-2} s^{-1} day^{-1})	0.2993	1.2801	0.5999	0.8854	0.7259
Photosynthesis recession velocity (V_f, μmol m^{-2} s^{-1} day^{-1})	0.3271	0.7895	0.3800	0.4786	0.5384
Photosynthesis upturn day (PUD)	133	149	105	116	140
Photosynthesis stabilization day (PSD)	169	166	149	143	164
Spring linear period (days)	36	17	44	27	24
Photosynthesis downturn day (PDD)	255	261	225	257	255
Photosynthesis recession day (PRD)	293	275	296	307	288
Fall linear period (days)	38	14	71	50	33

The capacity of vegetation to assimilate CO_2 over the growing season, as indicated by the growing season assimilation potential index (u), depends on not only the length of the growing season, but also how fast the vegetation can grow to its peak assimilation status and how long the vegetation can stay in its peak status. Comparing the Scots pine forest in Finland with the Aspen forest in Canada and Harvard Forest, the Scots pine forest has a smaller capacity to assimilate CO_2 during the growing season than either the aspen forest or Harvard Forest. However, it has a longer growing season: 187 days vs. 128 days for the aspen forest and 168 days for Harvard Forest. Its seasonal carbon assimilation capacity is limited by its small effective daily max. canopy photosynthetic rate: 18.5 μmol/m^2 s vs. 24.7 μmol/m^2 s for the

aspen forest and 27.1 μmol/m^2 s for Harvard Forest. Such differences between forests dominated by deciduous trees and those with evergreen species may reflect different strategies for maximizing potential use of environmental conditions.

It is interesting to note that while the length of the growing season as well as the days when the growing season starts or terminates differ a lot among different sites, the center of the growing seasons are quite close to each other among different sites. For example, the growing seasons start 43 days apart and end 32 days apart and their lengths of the growing season differ in 65 days, but their center of the growing season is only eight days apart.

Of fundamental importance are the vegetation photosynthesis development velocity in the spring and recession velocity in the fall. They indicate how quickly the vegetation can respond to changes in climatic conditions. For different vegetation types, the two velocities tend to be linearly related to each other ($V_f = 0.1484 + 0.4673V_s$, R^2 = 0.88, Figure 3), indicating that the rate of decline in the fall is proportional to the rate of development and expansion in the spring. In addition, vegetation photosynthesis tends to develop faster than it recesses.

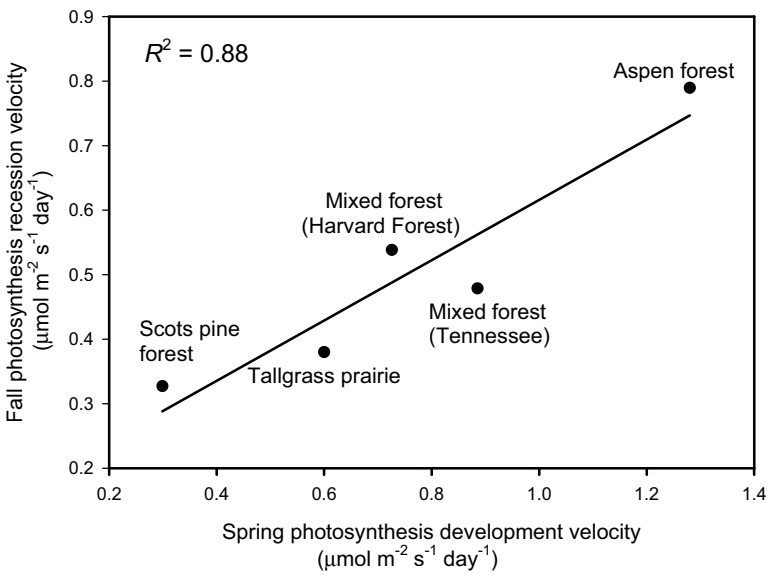

Figure 7.2-3. Relationship between photosynthesis development velocity and photosynthesis recession velocity.

7. CONCLUSIONS

In this chapter, we expanded the traditional research area of plant phenology by characterizing plant community growth activities from vegetation photosynthesis. We introduced a systematic approach to objectively determine the various stages in the seasonal march of vegetation photosynthesis. We derived a suite of phenological indices that can be used to describe seasonal vegetation photosynthetic activities for a variety of vegetation types. These indices make it possible to quantify the differences and similarities between different vegetation types in their responses to changes in climatic conditions. Our study indicates that vegetation functional types may be considered as basic units in phenological studies. We found that the pace of photosynthesis development in the spring is related to the pace of photosynthesis recession in the fall, and development is in general faster than recession.

The potential applications of these indices are tremendous. Studies indicate that global warming has been lengthening the growing season on global scales (e.g., Peñuelas and Filella 2001, Myneni et al. 1997) and variations in biospheric growth activities have been used to explain the interannual variability in atmospheric CO_2 concentration (Keeling et al. 1996). In these studies, biospheric growth activities are generally defined by changes in plant organs or vegetation greenness conditions. As we have demonstrated here, a longer growing season does not necessarily means larger CO_2 assimilation by vegetation. How fast plants reach their peak CO_2 assimilation potentials after released from winter dormancy is also important. If global warming reduces the velocity of spring photosynthesis development, the enhancement of annual carbon assimilation due to a lengthening growing season may be compromised. If the spring photosynthesis development velocity is reduced too much, then annual carbon assimilation can be adversely affected. In this case, the effective length of the growing season would provide a better measure for the effects of global warming on plant growth activities.

Future phenological research activities for the canopy photosynthetic indices proposed in this chapter would be to study how variable climatic conditions affect the expression of the indices. This would allow us to develop better models to predict impacts of global climate change on vegetation activities. Also there is a need to establish relationships between phenology of vegetation photosynthesis and traditional plant phenology. With such relationships, we can use the historical data of plant phenological observations to examine how vegetation photosynthesis has changed in the past.

This chapter essentially defines the growing season in the context of plant community CO_2 assimilation. Traditionally, growing seasons have been determined based on structural changes in plants (bud break, leaf-out, leaf fall, etc.). These two approaches might not always agree with each other as environmental factors such as frost, drought, insect activities, etc. affect plant photosynthesis. Clearly, however, to explain photosynthetic patterns as characterized by the indices developed in this chapter, it is necessary to link them with dynamics in canopy structures such as leaf area development. This is an issue that future studies should also address.

ACKNOWLEDGEMENTS

This study was initially conceived when L. Gu was working for Fluxnet at University of California at Berkeley. The bulk of the research was carried out at Oak Ridge National Laboratory (ORNL) with support from the U.S. Department of Energy, Office of Science, Biological and Environmental Research Program, Environmental Science Division, Terrestrial Carbon Program. We would like to thank Peter Curtis, Paul Hansen, Stan Wullschleger and Rich Norby for their comments on a draft of this chapter. ORNL is managed by UT-Battelle, LLC, for the U.S. Department of Energy under contract DE-AC05-00OR22725.

REFERENCES CITED

Aubinet, M., A. Grelle, A. Ibrom, Ü. Rannik, J. Moncrieff, T. Foken, A. S. Kowalski, P. H. Martin, P. Berbigier, C. Bernhofer, R. Clement, J. Elbers, A. Granier, T. Grünwald, K. Morgenstern, K. Pilegaard, C. Rebmann, W. Snijders, R. Valentini, and T. Vesala, Estimates of the annual net carbon and water exchanges of forests: The EUROFLUX methodology, *Advances in Ecological Research, 30*, 114-175, 2000.

Baldocchi, D. D., E. Falge, L. Gu, R. Olson, D. Hollinger, S. Running, P. Anthoni, C. Bernhofer, K. Davis, J. Fuentes, A. Goldstein, G. Katul, B. Law, X. Lee, Y. Malhi, T. P. Meyers, J. W. Munger, W. Oechel, K. Pilegaard, H. P. Schmid, R. Valentini, S. Verma, T. Vesala, K. Wilson, and S. Wofsy, FLUXNET: A new tool to study the temporal and spatial variability of ecosystem-scale carbon dioxide, water vapor and energy flux densities, *Bull. Amer. Meteorol. Soc., 82*, 2415-2435, 2001.

Baldocchi, D. D., B. B. Hicks, and T. P. Meyers, Measuring biosphere-atmosphere exchanges of biologically related gases with micrometeorological methods, *Ecology, 69*, 1331-1340, 1988.

Bradley, N. L., A. C. Leopold, J. Ross, and W. Huffaker, Phenological changes reflect climate change in Wisconsin, *Proc. Natl. Acad. Sci. (USA), 96*, 9701-9704, 1999.

Chmielewski, F. -M, The International Phenological Gardens across Europe: Present state and perspective, *Phenol. Seasonality, 1*, 19-23, 1996.

Fitzjarrald, D. R., O. C. Acevedo, and K. E. Moore, Climatic consequences of leaf presence in the eastern United States, *J. Climate, 14*, 598-614, 2001.

Freedman, J. M., D. R. Fitzjarrald, K. E. Moore, and R. K. Sakai, Boundary-layer clouds and vegetation-atmosphere feedbacks, *J. Climate, 14*, 180 – 197, 2001.

Goulden, M. L., J. W. Munger, S. –M. Fan, and B. C. Daube, Measurements of carbon sequestration by long-term eddy covariance: methods and a critical evaluation of the accuracy, *Global Change Biology, 2*, 169-182, 1996.

Gu, L., D. D. Baldocchi, S. B. Verma, T. A. Black, T. Vesala, E. M. Falge, and P. R. Dowty, Advantages of diffuse radiation for terrestrial ecosystem productivity, *J. Geophysical Research, 107(D6)*, DOI 10.1029/2001JD001242, 2002.

Keeling, C. D., J. F. S. Chin, and T. P. Whorf, Increased activities of northern vegetation inferred from atmospheric CO_2 measurements, *Nature, 382*, 146-149, 1996.

Lieth, H. (editor), *Phenology and Seasonality Modeling,* Spring-Verlag, New York, 444 pp., 1974.

Menzel, A., and P. Fabian, Growing season extended in Europe, *Nature*, 397, 659, 1999.

Mott, J. J., and A. J. Mccomb, Role of photoperiod and temperature in controlling phenology of 3 annual species from an arid region of western-Australia, *J. Ecology, 63*, 633-641, 1975.

Myneni, R. B., C. D. Keeling, C. J. Tucker, G. Asrar, and R. R. Nemani, Increased plant growth in the northern high latitudes from 1981 to 1991, *Nature, 386*, 698-702, 1997.

Peñuelas, J., and I. Filella, Responses to a warming world, *Science, 294*, 793-795, 2001.

Podolsky, A. S., *New Phenology: Elements of Mathematical Forecasting in Ecology*, John Wiley & Sons, New York, 504 pp., 1984.

Schwartz, M. D., and T. M. Crawford, Detecting energy balance modifications at the onset of spring, *Phys. Geography, 22*, 394-409, 2001.

Schwartz, M. D., Monitoring global change with phenology: The case of the spring green wave, *Int. J. Biometeorol.*, 38, 18-22, 1994.

Spano, D., C. Cesaraccio, P. Duce, and R. L. Snyder, Phenological stages of natural species and their use as climate indicators, *Int. J. Biometeorol., 42*, 124-133, 1999.

Suárez-López, P., K. Wheatley, F. Robson, H. Onouchi, F. Valverde, and G. Coupland, CONSTANS mediates between the circadian clock and the control of flowering in Arabidopsis, *Nature, 410*, 1116-1120, 2001.

Thomas, G. B., and R. L. Finney, R. L., Calculus and Analytic Geometry, 1139 pp., Addison-Wesley Publishing Company, Reading, Massachusetts, 1998.

Yanovsky, M. J., and S. A. Kay, Molecular basis of seasonal time measurement in Arabidopsis. *Nature, 419*, 308-312, 2002.